

Volume effects on the QCD critical end point from thermal fluctuations within the super statistics framework

Jorge David Castaño-Yepes,^{1,*} Fernando Martínez Paniagua,² Víctor Muñoz-Vitelly,³ and Cristian Felipe Ramirez-Gutierrez^{2,4}

¹*Instituto de Física, Pontificia Universidad Católica de Chile, Vicuña Mackenna 4860, Santiago, Chile.*

²*Ingeniería Física, Facultad de Ingeniería, Universidad Autónoma de Querétaro, C.P. 76010 Querétaro, Qro., Mexico.*

³*Instituto de Ciencias Nucleares, Universidad Nacional Autónoma de México, Apartado Postal 70-543, México Distrito Federal 04510, Mexico.*

⁴*Universidad Politécnica de Querétaro, El Marqués, 76240 Querétaro, Mexico.*

We investigate the impact of the finite volume and the thermal fluctuations on the Critical End Point of the QCD phase diagram. To do so, we implement the super statistics framework with Gamma distribution and its relation with the Tsallis non-extensive thermodynamics. We compute an effective thermodynamic potential as a function of the inverse temperature fluctuations and explicit dependence on the system volume. To find an analytic expression for the effective potential, we expand the modified Boltzmann factor by using the equilibrium thermodynamic potential computed in the Linear Sigma Model coupled to quarks. We find that the pseudo-critical temperature of transition at vanishing baryon chemical potential is modified by the size of the system being about 20% lower for small volumes. Additionally, the critical endpoint moves to higher densities and lower temperatures (about 12% in both cases). Interestingly, the results are quantitatively the same when the parameter that models the out-of-equilibrium situation is modified, indicating that the chiral symmetry restoration is robust against the thermal fluctuations in this approximation.

I. INTRODUCTION

In the understanding of the strongly interacting matter under extreme conditions, the study of the QCD-phase diagram has become of great interest in the last few years. In particular, determining the location of the Critical End Point (CEP) in the baryon chemical potential (μ_B) and temperature (T) plane is a challenging goal from theoretical and experimental perspectives. Recall that the QCD degrees of freedom are the quarks and gluons, and given the non-Abelian structure of its Lagrangian, those fundamental particles exhibit two important features: asymptotic freedom and color confinement [1, 2]. Such inherent properties of QCD open the possibility of performing a perturbative treatment in the large-momentum-transfer processes where the coupling constant is small. Conversely, in the small-momentum-transfer region, the perturbative methods are useless (the coupling becomes strong), and several non-perturbative alternatives are used: lattice QCD (LQCD) [3, 4], Dyson-Schwinger equations [5, 6], Nambu-Jona-Lasinio (NJL) model [7, 8], Linear Sigma Model (L σ M) [9, 10], among others.

As the QCD demands, those models obey the fundamental symmetries of the theory, and it is well established that in some regions of density and temperature, the chiral symmetry is restored from the hadronic matter to the quark-gluon plasma phase (QGP): LQCD with 2+1 light flavors shows a transition in the T -axis as a crossover with a pseudo-critical temperature $T_c \simeq 150 - 156$ MeV [11–13]. Moreover, many theoretical and phenomenological models predict a first-order transition line in the low T and large μ_B region [14–19]. Hence, the pass from a second order phase transition regime to one of first order defines the CEP location.

Although the phenomenological description of the experi-

mental data assumes conditions close to ideal thermalization, it is well established that in a heavy-ion collision, there are stages where the thermal equilibrium cannot be demanded a priori [20–22]. Indeed, the QGP-phase is preceded by the Glasma, which corresponds to a high gluon occupation system where its constituents are out of thermal equilibrium [23–25]. Previous works have demonstrated that the signals of the glasma can be relevant to the final observables such as elliptic flow and photon invariant momentum distribution [26–29]. Then, it is interesting to inquire if the non-equilibrium stages related to the QGP formation may modify the findings about the chiral symmetry restoration.

As an attempt to describe situations outside of thermal equilibrium, Super statistics (SS) is one of the most attractive frameworks for describing the non-equilibrium dynamics of complex systems. Beck and Cohen introduced the SS as an extension of the equilibrium Boltzmann statistics by considering fluctuations in some extensive parameter $\tilde{\beta}$ [30–32]. Such a parameter can be identified as the inverse temperature, vorticity, friction constant, volatility in finance, or a quantity whose space-time fluctuations are much larger than the typical relaxation time of the local dynamics. Previous works have shown that a SS description of the temperature and baryon chemical potential impact the CEP location [33, 34]. On the other hand, particular choices of SS are related to non-extensive thermodynamic scenarios [35, 36], so that SS may serve as a link between the thermal fluctuations and the studies with non-extensive statistical mechanics [37–39] or explicit volume dependence [40–42].

This work presents the interplay between the thermal fluctuations and the finite-volume effects in the CEP location in the L σ M framework. First, the out-of-equilibrium situation is modeled with the χ^2 distribution function so that the fluctuations of the inverse temperature β are encoded in the parameter q . The CEP's volume dependence arises from the definition of the Boltzmann partition function, which enters explicitly into the SS-thermodynamic potentials within a Tsallis-like

* Corresponding author: jcastano@uc.cl

prescription. The paper is organized as follows: In Sec. II, we present a summary of the SS and its relation with the non-extensive Tsallis thermodynamics. Next, in Sec. III, the SS-effective potential density is found in its general form as a function of its equilibrium counterpart. Then, in Sec. V, we present the effective density potential (in equilibrium) from the L σ M coupled to quarks. The results and discussion are presented in Sec. VI. Finally we summarize and give an outlook of the analysis in Sec. VII.

II. SUPER STATISTICS

The SS is based on the idea that some intensive parameter $\tilde{\beta}$ may fluctuate by following a certain probability distribution function $f(\tilde{\beta})$. By assuming that the system passes through equilibrium states $e^{-\tilde{\beta}\hat{H}}$, it is possible to construct a modified Boltzmann factor from the superposition of two statistics: one referring to the local equilibrium, and other due the fluctuations. Explicitly, this modified Boltzmann factor reads:

$$\hat{B} \equiv \int_0^\infty d\tilde{\beta} f(\tilde{\beta}) e^{-\tilde{\beta}\hat{H}}, \quad (1)$$

where \hat{H} is the Hamiltonian of the system. At this level, SS is an ansatz, and therefore, it cannot be taken as an first principles model for thermodynamic fluctuations.

Several models for $f(\tilde{\beta})$ are used, depending of the physical situation to be modeled. For example, the most used are:

- **Uniform distribution:** It is the simplest distribution, given by

$$f(\tilde{\beta}) = \frac{1}{b}, \quad (2)$$

with b a constant.

- **Multi-level distribution:** This distribution may appear when the system passes through several stages of Boltzmann-like equilibrium, each with equal probability. Its mathematical form is:

$$f(\tilde{\beta}) = \frac{1}{N} \sum_{k=1}^N \delta(\tilde{\beta} - \beta_k). \quad (3)$$

- **Gamma distribution:** The Gamma or χ^2 distribution is given by

$$f(\tilde{\beta}) = \frac{1}{b\Gamma(c)} \left(\frac{\tilde{\beta}}{c}\right)^{c-1} e^{-\tilde{\beta}/b}, \quad (4)$$

where b and c are free parameters.

- **Log-normal distribution:** This distribution function is given by

$$f(\tilde{\beta}) = \frac{1}{\sqrt{2\pi}u} \exp\left[-\frac{\log^2\left(\frac{\tilde{\beta}}{v}\right)}{2u^2}\right], \quad (5)$$

where u and v are free parameters.

- **F-distribution:** For positive integers v , and w and $b > 0$, the F-distribution is defined as:

$$f(\tilde{\beta}) = \frac{\Gamma[(v+w)/2]}{\Gamma(v/2)\Gamma(w/2)} \left(\frac{bv}{w}\right)^{v/2} \frac{\tilde{\beta}^{v/2-1}}{\left(1 + \frac{bv}{w}\tilde{\beta}\right)^{(v+w)/2}}. \quad (6)$$

The latter gives the Tsallis distribution in the $\tilde{\beta}$ -space when $v \rightarrow 2$.

In this work, in order to obtain analytical results for \hat{B} , we use the gamma-distribution function. An interesting case is provided when its parameters are chosen as

$$bc = \beta = 1/(k_B T), \text{ and } c = 1/(1-q), \quad (7)$$

so that \hat{B} can be written in terms of a q -exponential, namely:

$$\hat{B}(\beta) = e_q^{-\beta\hat{H}}, \quad (8)$$

where the q -exponential is defined as

$$e_q^x \equiv [1 + (1-q)x]^{1/(1-q)}. \quad (9)$$

From Eq. (8) it is possible to define a density operator as follows:

$$\hat{\rho} = \frac{1}{\mathcal{Z}} e_q^{-\beta\hat{H}}, \quad (10)$$

where \mathcal{Z} is the partition function given by

$$\mathcal{Z} = \text{Tr}\hat{\rho}, \quad (11)$$

and from which the thermodynamic properties can be defined. In particular, in order to describe the QCD chiral symmetry restoration, we are interested in the L σ M effective potential density which is described in the next section.

III. SUPER STATISTICAL EFFECTIVE POTENTIAL DENSITY

As is pointed out in previous works, one can explore the similarities of Eq. (8) within the non-additive Tsallis thermodynamics [35, 36]. The idea consists in preserving the Legendre structure (LS) of thermodynamics, which is lost in the Boltzmann-like formulation when the q -exponential is involved [43]. In the Tsallis prescription, the effective potential density is given by

$$\Omega_T = -\frac{1}{V\beta} \ln_q \mathcal{Z}, \quad (12)$$

where the subscript ‘‘T’’ is for Tsallis, and $\ln_q x$ is the q -logarithm, defined as:

$$\ln_q x = \frac{x^{1-q} - 1}{1-q}. \quad (13)$$

Preservation of LS is a desirable feature of a thermodynamic theory, because it is related to an increasing entropy and positive definite specific heat [44–46].

IV. SUPER STATISTICAL PARTITION FUNCTION

In order to find an expression for the SS-partition function, we expand Eq. (11) around $q = 1$, so that up to order $\mathcal{O}(q^2)$:

$$\mathcal{Z} \approx \mathcal{Z}_0 + \frac{q-1}{2} \beta^2 \frac{\partial^2 \mathcal{Z}_0}{\partial \beta^2} + \frac{(q-1)^2}{24} \left(3\beta^4 \frac{\partial^4 \mathcal{Z}_0}{\partial \beta^4} + 8\beta^3 \frac{\partial^3 \mathcal{Z}_0}{\partial \beta^3} \right), \quad (14)$$

where \mathcal{Z}_0 is the Boltzmann partition function given by:

$$\mathcal{Z}_0 = \exp(-V\beta\Omega_0), \quad (15)$$

where Ω_0 is the equilibrium effective potential density, and V is the volume of the system.

Note that the derivatives of \mathcal{Z}_0 introduce a non-trivial volume dependence, namely,

$$\mathcal{Z} \approx e^{-\beta V \Omega_0} \left[1 + \frac{q-1}{2} (\beta V \Omega_0)^2 + \frac{(q-1)^2}{24} (\beta V \Omega_0)^3 (3\beta V \Omega_0 + 8) \right]. \quad (16)$$

The latter partition function has two interesting features: it includes thermal fluctuations within the q -parameter, and links the non-extensive scenario with an explicit volume dependence. Then, the effective potential reads:

$$\Omega_T = \frac{1}{(q-1)V\beta} \left\{ e^{-(1-q)V\beta\Omega_0} \left[1 + \frac{q-1}{2} (\beta V \Omega_0)^2 + \frac{(q-1)^2}{24} (\beta V \Omega_0)^3 (3\beta V \Omega_0 + 8) \right]^{1-q} - 1 \right\}, \quad (17)$$

so that in the limits $q \rightarrow 1$, $V \rightarrow \infty$ potential Ω_0 is obtained.

V. EQUILIBRIUM EFFECTIVE POTENTIAL OF LINEAR SIGMA MODEL COUPLED TO QUARKS

In Sec. IV, the SS effective potential density is written in terms of the equilibrium potential Ω_0 . To obtain it, and in order to compute some features of the QCD phase diagram,

we use the LSMq whose Lagrangian density is given by [18]:

$$\mathcal{L} = \frac{1}{2}(\partial_\mu \sigma)^2 + \frac{1}{2}(\partial_\mu \boldsymbol{\pi})^2 + \frac{a^2}{2}(\sigma^2 + \boldsymbol{\pi}^2) - \frac{\lambda}{4}(\sigma^2 + \boldsymbol{\pi}^2)^2 + i\bar{\psi}\gamma^\mu \partial_\mu \psi - g\bar{\psi}(\sigma + i\gamma_5 \boldsymbol{\tau} \cdot \boldsymbol{\pi})\psi, \quad (18)$$

where the mass parameter a^2 , and the couplings λ and g are positive constants, ψ is an SU(2) isospin doublet, and $\boldsymbol{\pi}$ and σ are an isospin triplet and singlet, respectively. We take the neutral pion π^0 as the third component of the triplet, and the charged pions as

$$\pi_\pm = \frac{1}{2}(\pi_1 \mp i\pi_2). \quad (19)$$

It is well established that this model admits spontaneous symmetry breaking, which can be realized over the σ field when it develops a vacuum expectation value v . This mechanism is obtained from the shift:

$$\sigma \rightarrow \sigma + v, \quad (20)$$

so that

$$\begin{aligned} \mathcal{L} = & \frac{a^2}{2}v^2 - \frac{\lambda}{4}v^4 \\ & - \frac{1}{2}(\partial_\mu \sigma)^2 - \frac{1}{2}(3\lambda v^2 - a^2)\sigma^2 \\ & - \frac{1}{2}(\partial_\mu \boldsymbol{\pi})^2 - \frac{1}{2}(\lambda v^2 - a^2)\boldsymbol{\pi}^2 \\ & + i\bar{\psi}\gamma^\mu \partial_\mu \psi - gv\bar{\psi}\psi + \mathcal{L}_I^b + \mathcal{L}_I^f \end{aligned} \quad (21)$$

where

$$\mathcal{L}_I^b = -\frac{\lambda}{4}(\sigma^2 + \boldsymbol{\pi}^2)^2, \quad (22a)$$

and

$$\mathcal{L}_I^f = -g\bar{\psi}(\sigma + i\gamma_5 \boldsymbol{\tau} \cdot \boldsymbol{\pi})\psi. \quad (22b)$$

The latter equations implies that after symmetry breaking, the involved fields acquire mass given by

$$m_\sigma^2 = 3\lambda v^2 - a^2, \quad (23a)$$

$$m_\pi^2 = \lambda v^2 - a^2, \quad (23b)$$

$$m_f^2 = gv. \quad (23c)$$

To compute the equilibrium effects of the finite temperature and density in the chiral symmetry restoration, we use the effective potential and the self-energy up to the ring diagrams, so that in a high-temperature limit where the quark masses are small, they are [10, 18]:

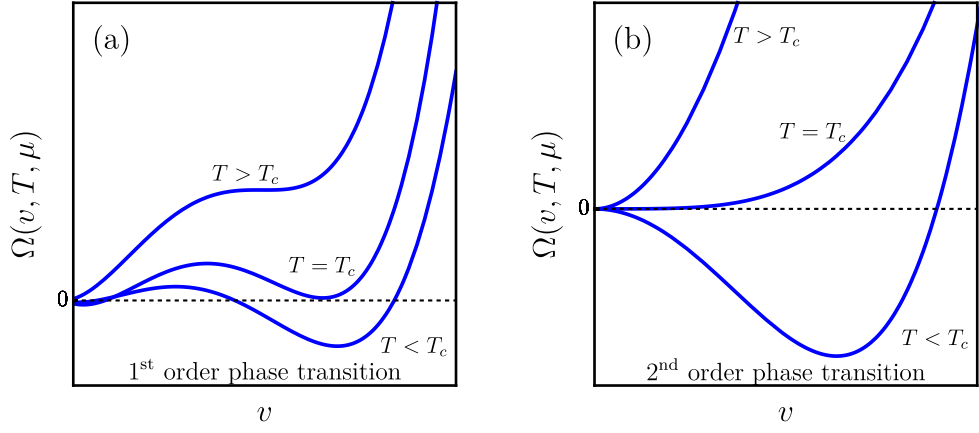


FIG. 1. Shapes of the effective potential as function of the order parameter v and for temperatures lowers, equal, and higher than the transition temperature T_c .

$$\begin{aligned} \Omega_0 = & -\frac{a^2}{2}v^2 + \frac{\lambda}{4}v^4 + \sum_{i=\sigma,\pi} \left\{ \frac{m_i^4}{64\pi^2} \left[\ln \left(\frac{16\pi^2 T^2}{2a^2} \right) - 2\gamma_e + 1 \right] - \frac{\pi^2 T^4}{90} + \frac{m_i^2 T^2}{24} - \frac{T}{12\pi} [m_i^2 + \Pi(T, \mu)]^{3/2} \right\} \\ & - \frac{N_c}{16\pi^2} \sum_{f=u,d} \left\{ m_f^4 \left[\ln \left(\frac{8\pi^2 T^2}{a^2} \right) + \psi_0 \left(\frac{1}{2} + \frac{i\mu}{2\pi T} \right) + \psi_0 \left(\frac{1}{2} - \frac{i\mu}{2\pi T} \right) + 1 \right] + 8m_f^2 T^2 \left[\text{Li}_2 \left(-e^{\mu/T} \right) \right. \right. \\ & \left. \left. + \text{Li}_2 \left(-e^{-\mu/T} \right) \right] - 32T^4 \left[\text{Li}_4 \left(-e^{\mu/T} \right) + \text{Li}_4 \left(-e^{-\mu/T} \right) \right] \right\}, \end{aligned} \quad (24)$$

and

$$\begin{aligned} \Pi(T, \mu) = & \frac{\lambda T^2}{2} \\ & - \frac{N_f N_c g^2 T^2}{\pi^2} \left[\text{Li}_2 \left(-e^{\mu/T} \right) + \text{Li}_2 \left(-e^{-\mu/T} \right) \right], \end{aligned} \quad (25)$$

where γ_e is the Euler-Mascheroni constant, $\psi_0(x)$ is the digamma function, and $\text{Li}_n(x)$ is the poly-logarithm function of order n . Moreover, we take $N_c = 3$ and $N_f = 2$, as the number of colors and flavors, respectively. The coupling constants are fixed with conditions at $\mu = 0$, where the physical boson masses (corrected by the self-energy) are:

$$m_\sigma^2 = 3\lambda v^2 - a^2 + \frac{\lambda T^2}{2} + \frac{N_f N_c g^2 T^2}{6}, \quad (26a)$$

and

$$m_\pi^2 = \lambda v^2 - a^2 + \frac{\lambda T^2}{2} + \frac{N_f N_c g^2 T^2}{6}, \quad (26b)$$

so that in the transition temperature T_c , the masses vanishes. The, by solving for a from Eqs. (26):

$$a = T_c \sqrt{\frac{\lambda}{2} + \frac{N_f N_c g^2}{6}}. \quad (27)$$

Now, from Eqs. (23) is easy to check that:

$$a = \sqrt{\frac{m_\sigma^2 - 3m_\pi^2}{2}} \quad (28)$$

The present work takes into account only two quark flavors in the chiral limit, which allows to compare with lattice simulations for $N_f = 2 + 1$, where the critical temperature at $\mu = 0$ is $T \simeq 170$ MeV [47]. Then, the constants λ and g can be identified, and throughout the paper, we take them as $\lambda = 0.86$, and $g = 1.1$.

Our goal is to describe the chiral symmetry restoration where the quark mass vanishes so that the sigma's field vacuum expectation value v is promoted as the order parameter for the transition. In that spirit, the phase transition and its order are identified from the effective potential shape in such a way that the order parameter has a discontinuity at the critical temperature T_c for a first order phase transition. In contrast, in a second-order phase transition, it evolves continuously. Figure 1 illustrates the potential shape for both situations.

VI. RESULTS AND DISCUSSION

In the previous sections, we developed a formalism to describe the QCD chiral symmetry restoration within the $L\sigma M$ coupled to quarks when the system has fluctuations in its temperature. Moreover, given the connection between SS and the Tsallis non-additive thermodynamics, our formalism links the out-of-equilibrium situation with an explicit volume dependence. This section explores the impact of thermal fluctuations and the system's size in the CEP location and the transition lines.

Before presenting our results, let us comment that the parameters q and V are independent. This is an important feature because the SS formalism can be interpreted as if the system is divided into N subsystems, each with local equilibrium, and the distribution function $f(\tilde{\beta})$ accounts for the spatial temperature distribution among them [32–34]. The latter implies that the q -parameter can be identified as:

$$q = 1 + 2/N. \quad (29)$$

Nevertheless, there is another interpretation of the SS: the system is not divided into subsystems, but it as a whole passes through several equilibrium stages. Then, the total volume remains unaltered, and the fluctuations acquire a temporal nature. We adopt this point of view.

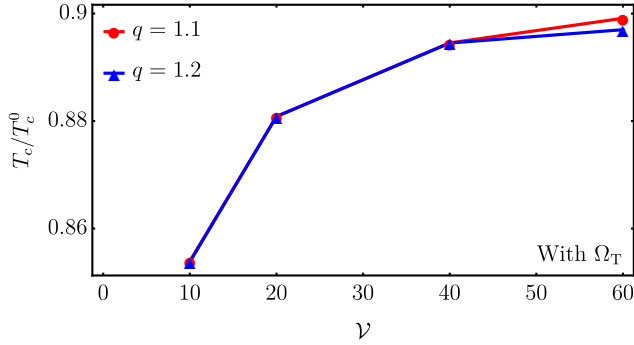


FIG. 2. Pseudo-critical temperature T_c at $\mu = 0$, as a function of the dimensionless volume $\mathcal{V} = a^3 V$ for $q = 1.1$ and $q = 1.2$. The reference temperature T_c^0 is the transition temperature at $\mu = 0$ in the equilibrium case $q \rightarrow 1$. The curves are obtained with the Tsallis prescription. A similar behavior is found with $q = 0.8$, and $q = 0.9$.

On the other hand, given that the SS is an ansatz, the q -parameter can be interpreted in several ways beyond the relation of Eq. (29). In fact, this parameter can be related to the variance of the inverse temperature fluctuations [30]:

$$(q - 1)\beta^2 = \sigma^2 \text{ or } q = \frac{\langle \tilde{\beta}^2 \rangle}{\langle \tilde{\beta} \rangle^2}, \quad (30)$$

so that it is possible to find a general expression for the modified Boltzmann factor given by:

$$\hat{B} = e^{-\beta \hat{H}} \left[1 + \frac{1}{2} \sigma^2 \hat{H}^2 + \mathcal{O}(\sigma^3 \hat{H}^3) \right], \quad (31)$$

where the variances (and therefore, the q -parameter) have different forms. For example, for the uniform, log-normal, and the F-distribution, the variances are respectively:

$$\sigma^2 = b^2/12, \quad (32a)$$

$$\sigma^2 = v^2 e^{s^2} (e^{s^2} - 1), \quad (32b)$$

and

$$\sigma^2 = \frac{2w^2(v+w-2)}{b^2 v(w-2)^2(w-4)}. \quad (32c)$$

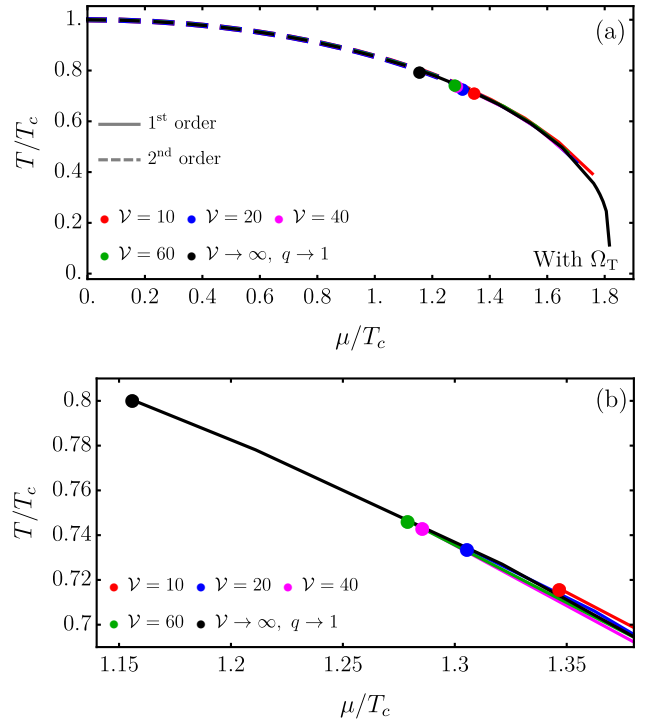


FIG. 3. Effective QCD phase diagram obtained from the potential Ω_T for $q = 1.2$ and several values of \mathcal{V} . The points are the CEP's location for each volume. The values of T and μ in the critical line are normalized to their own T_c which is volume-dependent. Panel (a) is the full phase diagram, and panel (b) is a zoom in order to appreciate the volume effects in the CEP (only the first-order critical lines are shown.).

Hence, in order to present general results, we explore the range $0.8 \leq q \leq 1.2$ (values outside of this interval imply more terms in the series expansion).

Figure 2 shows the pseudo-critical temperature T_c (at $\mu_B = 0$) as a function of the thermal fluctuation's parameter q , and the dimensionless volume $\mathcal{V} \equiv a^3 V$. In order to visualize the effects of the variables, we scaled T_c with the pseudo-critical temperature at thermal equilibrium T_c^0 . As can be noticed, the fluctuations in temperature reproduce almost the same results for $q = 1.1$ and $q = 1.2$ (the same behavior is found with $q = 0.8$, and $q = 0.9$). Still, for small system size, the transition temperature decreases around 20% from the value found in the equilibrium situation. Note that a similar scaling with the volume is found in Ref. [40] for a finite box model by using lattice Yang–Mills theory and Dyson–Schwinger equations for 2+1 quark flavors.

Figure 3 presents the effective QCD phase diagram in the plane $\mu - T$ (recall $\mu_B = 3\mu$) computed from Eq. (17) for several values of \mathcal{V} with $q = 1.2$. The dashed curves represent the crossover or second-order phase transition lines, whereas the continuous are the first-order critical regions. The dots are the CEP location when the critical values of T and μ are scaled with the respective T_c for each \mathcal{V} . The finite volume effect is translated to move the the CEP toward smaller temperatures and larger chemical potentials, which correspond to a

change about 10%-17% for μ , and 10%-12% for T . Again, the findings are in agreement with the findings of with Ref. [40]. Moreover, the results are quantitatively the same when variations in q are implemented, which indicates that the transition lines and the CEP location are robust against thermal fluctuations but have a considerable dependence on the size of the system.

VII. SUMMARY AND CONCLUSIONS

In this work, we have used the $L\sigma M$ coupled with quarks to locate the CEP in the effective QCD phase diagram by considering the finite-size effects produced by thermal fluctuations. The SS provides the connection between the out-of-equilibrium condition and the non-extensive thermodynamics with the χ^2 -distribution function so that its free parameters resemble the Tsallis statistics. Therefore, we end with an effective thermodynamic potential as a function of the thermal fluctuations parameter q and explicit volume dependence. To appreciate the finite size effects, we adopted the SS interpretation in which the distribution function models the system as a whole, passing for several stages close to the thermal equilibrium. Moreover, given the universality of the modified Boltz-

mann factor, we expanded the range of values of q by demanding its nature as a parameter into an ansatz. With this, several distribution functions can be considered.

We find that the pseudo-critical temperature T_c at $\mu = 0$ is considerably changed when the system's volume decreases (around a 20% for the smaller volume considered). Nevertheless, the temperature fluctuations do not represent significant changes in the value of T_c . The same situation is found in the CEP location: it moves towards high values of μ and lower temperatures, so that the former may change in a range of the 10% – 17%, and the latter in the range of 10% – 12%, when the plane $\mu-T$ is scaled by the respective pseudo-critical temperatures for each volume. Furthermore, the critical lines for each set of parameters lie close to the curve of the equilibrium case. Interestingly, the named results are quantitatively the same when q varies in the interval $0.8 \leq q \leq 1.2$, which indicates that in this approximation, the chiral symmetry restoration is robust against the thermal fluctuations. Still, the order of the transition may be affected by the size of the system.

ACKNOWLEDGEMENT

We would like to thank Prof. A. Ayala for his useful comments and suggestions about this work.

-
- [1] David J. Gross and Frank Wilczek, "Ultraviolet behavior of non-abelian gauge theories," *Phys. Rev. Lett.* **30**, 1343–1346 (1973).
 - [2] H. David Politzer, "Reliable perturbative results for strong interactions?" *Phys. Rev. Lett.* **30**, 1346–1349 (1973).
 - [3] Michael Creutz, *Quarks, gluons and lattices*, Vol. 8 (Cambridge University Press, 1983).
 - [4] István Montvay and Gernot Münster, *Quantum fields on a lattice* (Cambridge University Press, 1997).
 - [5] Christian S. Fischer, "QCD at finite temperature and chemical potential from Dyson–Schwinger equations," *Prog. Part. Nucl. Phys.* **105**, 1–60 (2019).
 - [6] Philipp Isserstedt, Michael Buballa, Christian S. Fischer, and Pascal J. Gunkel, "Baryon number fluctuations in the QCD phase diagram from Dyson–Schwinger equations," *Phys. Rev. D* **100**, 074011 (2019).
 - [7] Lu-Meng Liu, Jun Xu, and Guang-Xiong Peng, "Three-dimensional QCD phase diagram with a pion condensate in the NJL model," *Phys. Rev. D* **104**, 076009 (2021).
 - [8] Alejandro Ayala, Luis A Hernández, Marcelo Loewe, and Cristian Villavicencio, "QCD phase diagram in a magnetized medium from the chiral symmetry perspective: the linear sigma model with quarks and the Nambu–Jona-Lasinio model effective descriptions," *Eur. Phys. J. A* **57**, 1–25 (2021).
 - [9] Alejandro Ayala, Bilgai Almeida Zamora, JJ Cobos-Martínez, S Hernández-Ortiz, LA Hernández, Alfredo Raya, and María Elena Tejada-Yeomans, "Collision energy dependence of the critical end point from baryon number fluctuations in the Linear Sigma Model with quarks," *EPJA* **58**, 1–10 (2022).
 - [10] Alejandro Ayala, Adnan Bashir, J.J. Cobos-Martínez, Saúl Hernández-Ortiz, and Alfredo Raya, "The effective QCD phase diagram and the critical end point," *Nucl. Phys. B* **897**, 77–86 (2015).
 - [11] Yasumichi Aoki, Z Fodor, SD Katz, and KK Szabo, "The QCD transition temperature: Results with physical masses in the continuum limit," *Phys. Lett. B* **643**, 46–54 (2006).
 - [12] Tanmoy Bhattacharya *et al.* (HotQCD Collaboration), "QCD Phase Transition with Chiral Quarks and Physical Quark Masses," *Phys. Rev. Lett.* **113**, 082001 (2014).
 - [13] A. Bazavov *et al.* (HotQCD Collaboration), "Chiral and deconfinement aspects of the QCD transition," *Phys. Rev. D* **85**, 054503 (2012).
 - [14] A. Barducci, R. Casalbuoni, S. De Curtis, R. Gatto, and G. Pettini, "Chiral phase transitions in QCD for finite temperature and density," *Phys. Rev. D* **41**, 1610–1619 (1990).
 - [15] A. Barducci, R. Casalbuoni, G. Pettini, and R. Gatto, "Chiral phases of QCD at finite density and temperature," *Phys. Rev. D* **49**, 426–436 (1994).
 - [16] N. G. Antoniou, F. K. Diakonou, X. N. Maintas, and C. E. Tsagkarakis, "Locating the QCD critical endpoint through finite-size scaling," *Phys. Rev. D* **97**, 034015 (2018).
 - [17] Chiho Nonaka and Masayuki Asakawa, "Hydrodynamical evolution near the QCD critical end point," *Phys. Rev. C* **71**, 044904 (2005).
 - [18] Alejandro Ayala, Jorge David Castano-Yepes, JJ Cobos-Martínez, Saúl Hernández-Ortiz, Ana Julia Mizher, and Alfredo Raya, "Chiral symmetry transition in the linear sigma model with quarks: Counting effective QCD degrees of freedom from low to high temperature," *Int. J. Mod. Phys. A* **31**, 1650199 (2016).
 - [19] R. V. Gavai and Sourendu Gupta, "On the critical end point of QCD," *Phys. Rev. D* **71**, 114014 (2005).
 - [20] Wojciech Florkowski and Radoslaw Ryblewski, "Highly anisotropic and strongly dissipative hydrodynamics for early

- stages of relativistic heavy-ion collisions,” *Phys. Rev. C* **83**, 034907 (2011).
- [21] S. V. Akkelin and Yu. M. Sinyukov, “Matching of nonthermal initial conditions and hydrodynamic stage in ultrarelativistic heavy-ion collisions,” *Phys. Rev. C* **81**, 064901 (2010).
- [22] J.P. Blaizot and A.H. Mueller, “The early stage of ultrarelativistic heavy ion collisions,” *Nucl. Phys. B* **289**, 847–860 (1987).
- [23] T. Lappi and L. McLerran, “Some features of the glasma,” *Nucl. Phys. A* **772**, 200–212 (2006).
- [24] Naoto Tanji and Raju Venugopalan, “Effective kinetic description of the expanding overoccupied glasma,” *Phys. Rev. D* **95**, 094009 (2017).
- [25] Raju Venugopalan, “From glasma to quark–gluon plasma in heavy-ion collisions,” *JPhysG* **35**, 104003 (2008).
- [26] M Ruggieri, F Scardina, S Plumari, and V Greco, “Elliptic flow from non-equilibrium initial condition with a saturation scale,” *Phys. Lett. B* **727**, 177–181 (2013).
- [27] M. Ruggieri, F. Scardina, S. Plumari, and V. Greco, “Thermalization, isotropization, and elliptic flow from nonequilibrium initial conditions with a saturation scale,” *Phys. Rev. C* **89**, 054914 (2014).
- [28] Alejandro Ayala, Jorge David Castaño Yepes, C. A. Dominguez, L. A. Hernández, Saúl Hernández-Ortiz, and María Elena Tejeda-Yeomans, “Prompt photon yield and elliptic flow from gluon fusion induced by magnetic fields in relativistic heavy-ion collisions,” *Phys. Rev. D* **96**, 014023 (2017).
- [29] Alejandro Ayala, Jorge David Castaño-Yepes, Isabel Dominguez Jimenez, Jordi Salinas San Martín, and María Elena Tejeda-Yeomans, “Centrality dependence of photon yield and elliptic flow from gluon fusion and splitting induced by magnetic fields in relativistic heavy-ion collisions,” *EPJA* **56**, 1–11 (2020).
- [30] Christian Beck and Ezechiel G. D. Cohen, “Superstatistics,” *Phys. A* **322**, 267–275 (2003).
- [31] Christian Beck, “Superstatistics: theory and applications,” *Contin. Mech. Thermodyn.* **16**, 293–304 (2004).
- [32] Christian Beck, “Recent developments in superstatistics,” *Braz. J. Phys.* **39**, 357–363 (2009).
- [33] Alejandro Ayala, Martin Hentschinski, L. A. Hernández, M. Loewe, and R. Zamora, “Superstatistics and the effective QCD phase diagram,” *Phys. Rev. D* **98**, 114002 (2018).
- [34] Alejandro Ayala, Saul Hernández-Ortiz, L. A. Hernández, Víctor Knapp-Pérez, and R. Zamora, “Fluctuating temperature and baryon chemical potential in heavy-ion collisions and the position of the critical end point in the effective QCD phase diagram,” *Phys. Rev. D* **101**, 074023 (2020).
- [35] Jorge David Castaño Yepes and Cristian Felipe Ramirez-Gutierrez, “Superstatistics and quantum entanglement in the isotropic spin-1/2 XX dimer from a nonadditive thermodynamics perspective,” *Phys. Rev. E* **104**, 024139 (2021).
- [36] “Entropy exchange and thermal fluctuations in the Jaynes–Cummings model, author=Castaño-Yepes, Jorge David,” *EPJP* **137**, 1–14 (2022).
- [37] Ya-Peng Zhao, “Thermodynamic properties and transport coefficients of QCD matter within the nonextensive Polyakov–Nambu–Jona-Lasinio model,” *Phys. Rev. D* **101**, 096006 (2020).
- [38] Jacek Rozynek and Grzegorz Wilk, “Nonextensive nambu-jona-lasinio model of qcd matter,” *EPJA* **52**, 1–15 (2016).
- [39] Masamichi Ishihara, “Chiral phase transitions in the linear sigma model in the Tsallis nonextensive statistics,” *Int. J. Mod. Phys. E* **25**, 1650066 (2016).
- [40] Julian Bernhardt, Christian S. Fischer, Philipp Isserstedt, and Bernd-Jochen Schaefer, “Critical endpoint of QCD in a finite volume,” *Phys. Rev. D* **104**, 074035 (2021).
- [41] Bertram Klein, “Modeling finite-volume effects and chiral symmetry breaking in two-flavor QCD thermodynamics,” *Phys. Rep.* **707**, 1–51 (2017).
- [42] Jens Braun, Bertram Klein, and Bernd-Jochen Schaefer, “On the phase structure of QCD in a finite volume,” *Phys. Lett. B* **713**, 216–223 (2012).
- [43] Constantino Tsallis, Renio S. Mendes, and Anel R. Plastino, “The role of constraints within generalized nonextensive statistics,” *Phys. A* **261**, 534–554 (1998).
- [44] A. M. Scarfone, H. Matsuzoe, and T. Wada, “Consistency of the structure of Legendre transform in thermodynamics with the Kolmogorov–Nagumo average,” *Phys. Lett. A* **380**, 3022–3028 (2016).
- [45] A. Plastino and A. R. Plastino, “On the universality of thermodynamics’ Legendre transform structure,” *Phys. Lett. A* **226**, 257–263 (1997).
- [46] Jorge David Castaño-Yepes and D. A. Amor-Quiroz, “Superstatistical description of thermo-magnetic properties of a system of 2D GaAs quantum dots with gaussian confinement and Rashba spin–orbit interaction,” *Phys. A* **548**, 123871 (2020).
- [47] Y Maetzawa, S Aoki, S Ejiri, T Hatsuda, N Ishii, K Kanaya, and N Ukita, “Thermodynamics of two-flavour lattice QCD with an improved Wilson quark action at non-zero temperature and density,” *J. Phys. G: Nucl. Part. Phys.* **34**, S651–S654 (2007).